

A. A. Gowardhan<sup>1</sup>, M. J. Brown<sup>1</sup>, D.S. DeCroix<sup>1</sup> and E. R. Pardyjak<sup>2</sup><sup>1</sup>Los Alamos National Laboratory, Los Alamos, NM, <sup>2</sup>University of Utah, Salt Lake City, UT

## 1. INTRODUCTION

As part of the Quick Urban & Industrial Complex (QUIC) Dispersion Modeling System, a pressure solver has been developed to compute a 3D pressure field around buildings. The solver generates the pressure field by solving the pressure Poisson equation, obtained by taking the spatial divergence of the steady-state Navier-Stokes equations for incompressible flows. The input to the solver is the 3D mean wind field obtained from the QUIC-URB fast response urban wind model (Pardyjak and Brown, 2002). QUIC-URB generates a mass consistent mean wind field around buildings by using various empirical relationships for initializing the velocity fields in the regions around buildings (e.g. *upwind cavity, wake, street canyon, rooftop*) and then this initial flow field is forced to satisfy mass conservation (see Fig.1).

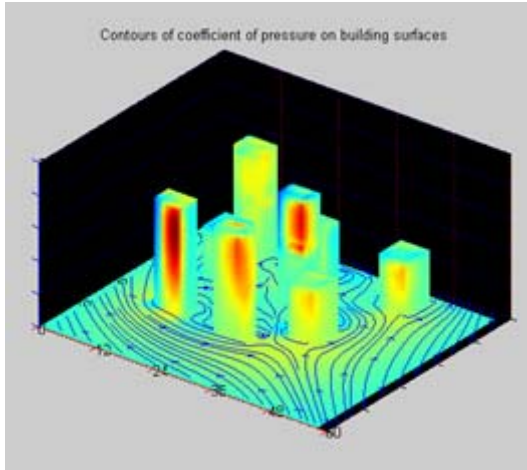


Fig. 1: QUIC-computed streamlines superimposed on pressure coefficient contours computed by the QUIC Pressure Solver.

## 2. MODEL DESCRIPTION AND SOLUTION PROCEDURE

The pressure Poisson equation is derived from the Reynolds-averaged Navier-Stokes (RANS) equations for incompressible flow without body forces, expressed here using Einsteinian notation as:

$$\frac{\partial \bar{U}_i}{\partial t} = -\frac{\partial(\bar{U}_i \bar{U}_j)}{\partial x_j} - \frac{1}{\rho} \frac{\partial \bar{P}}{\partial x_i} - \frac{\partial(\overline{u'_i u'_j})}{\partial x_j} + \nu \frac{\partial^2 \bar{U}_i}{\partial x_j \partial x_j} \quad (1)$$

where  $\bar{U}_i$  is the mean velocity in the  $x_i$  direction,  $u'_i$  is the turbulent fluctuating velocity,  $\bar{P}$  is the mean pressure,  $\rho$  is the average density,  $\overline{u'_i u'_j}$  is the Reynolds stress, and  $\nu$  is the kinematic viscosity.

Assuming steady-state conditions and taking the divergence of Eqn. (1), we obtain

$$\frac{\partial}{\partial x_i} \left( \frac{\partial \bar{P}}{\partial x_i} \right) = \rho \frac{\partial}{\partial x_i} \left( \nu \frac{\partial^2 \bar{U}_i}{\partial x_j \partial x_j} - \frac{\partial(\bar{U}_i \bar{U}_j)}{\partial x_j} - \frac{\partial(\overline{u'_i u'_j})}{\partial x_j} \right) \quad (2)$$

Equation (2) is the pressure Poisson equation. Since the QUIC-URB wind model only produces the mean wind field and produces no information on the turbulence, for the time being, we simplify the equation further by neglecting the Reynolds stresses. As will be discussed later, differences between the model-computed and measured pressure may be due to neglecting these terms. In the future, the Reynolds stresses will be included in the calculation, if a viable method for approximating their magnitude and spatial distribution from the mean flow can be obtained.

The QUIC Pressure Solver uses the Jacobi method to iteratively solve the pressure Poisson equation. A second-order accurate *central differencing* scheme has been used to obtain the source term for the pressure Poisson equation (R.H.S. of Eqn. (2)) at each grid point in the solution domain. At the west and south building faces, a first-order accurate *upwind differencing* scheme is used to calculate the source term and at the east and north faces, a first-order accurate *forward differencing* scheme is used.

At the building faces, the pressure field is obtained by solving the steady-state Reynolds-averaged Navier-Stokes equation in the direction normal to the wall. For example, for the face normal to the x-direction, the pressure field is obtained by solving:

$$\frac{\partial \bar{P}}{\partial x} = \rho \left( -\frac{\partial \bar{U}\bar{U}}{\partial x} - \frac{\partial \bar{U}\bar{V}}{\partial y} - \frac{\partial \bar{U}\bar{W}}{\partial z} + \nu \left[ \frac{\partial^2 \bar{U}}{\partial x^2} + \frac{\partial^2 \bar{U}}{\partial y^2} + \frac{\partial^2 \bar{U}}{\partial z^2} \right] \right) \quad (3)$$

\* Corresponding author address: Akshay Gowardhan, Los Alamos National Laboratory, Los Alamos, NM-87545, e-mail: [agowardhan@lanl.gov](mailto:agowardhan@lanl.gov)

The initial value of pressure at each grid point inside the solution domain was specified as the ambient atmospheric pressure. The boundary value was set to the atmospheric pressure (Dirichlet boundary condition). The computed pressure field is normalized by subtracting the ambient atmospheric pressure ( $\overline{P}_o$ ) and then by dividing by the free stream velocity ( $V_o$ ) at the reference height to obtain the coefficient of pressure ( $C_p$ ):

$$C_p = \frac{\overline{P} - \overline{P}_o}{\left(\frac{1}{2}\rho V_o^2\right)} \quad (4)$$

### 3. EXPERIMENTAL DESCRIPTION

The QUIC Pressure Solver has been evaluated using wind-tunnel data from cube, tall building, wide building, and multiple building experiments (Gowardhan et al., 2005). In this paper, comparisons were made with the wind tunnel data of Baines (1963) for a cubical building and a tall building with dimensions of 1:1:8 (length : width : height).

These wind-tunnel experiments were performed in the low-speed open-return wind tunnel of the Department of Mechanical Engineering at the University of Toronto. The tunnel has a cross-sectional area of 4 ft. by 8 ft. and a maximum speed of 25 ft. /sec. The model of the building was made of acrylic plastic sheet material. The cubical and tall building had a square floor plan and a height-to-width ratio of 1:1 and 1:8, respectively (Baines, 1963). Pressures were small and required the careful use of a micro manometer.

The experiments were conducted with uniform flow and boundary-layer flow. To produce a uniform flow around the building, the building model was placed on a thin ground board which was clear of the natural boundary layer of the wind-tunnel floor. For the case of sheared flow, a boundary-layer velocity profile was produced in the lower half of the wind tunnel by installing a curved screen in the entrance of the wind-tunnel test section. The shear inflow is represented by a power law with an exponent of 0.25:

$$u = u_{ref} \left( \frac{z}{z_{ref}} \right)^{0.25} \quad (5)$$

In addition, the pressure solver results were also compared to the ASHRAE's Handbook data (1985) and the LES simulation performed by Rehm et.al.(1999) for cubes.

## 4. RESULTS AND DISCUSSION

### i. Uniform flow normal to the cube face

The QUIC simulation of the cubical building was performed to match the conditions of the wind tunnel. The upwind cavity flag in QUIC-URB was turned off as an upwind cavity was not formed for the uniform flow case in the wind tunnel (Baines, 1963) and the rooftop flag for recirculation was turned on. The grid cell size was set to H/10, where H is the building height, and a uniform velocity of 5m/s was prescribed at the inlet. The reference height for normalizing pressure was taken as the building height (H).

Figure 2 shows the contours of coefficient of mean pressure generated by the QUIC Pressure Solver on the building surfaces and Fig. 3 shows the wind-tunnel measurements for the same case (Baines, 1963). Comparison of Figs. 2 and 3 indicates that the patterns of the pressure coefficient predicted by the QUIC Pressure Solver are nearly identical to those measured on the front face, while the magnitude of  $C_p$  is in reasonably good agreement, over predicting the maximum value by approximately 20%.

The contour patterns and the values of  $C_p$  predicted by the QUIC Pressure Solver on the sidewall face, however, are quite dissimilar. A broad region of large negative  $C_p$  exists in the measurements, with the maximum pressure deficit occurring at the downwind edge of the sidewall face. In contrast, the model computations show the maximum pressure deficit near the leading edge of the sidewall face and higher values of  $C_p$  on the downwind edge. Also, the values of negative  $C_p$  predicted by the model are substantially smaller than the experimental values. These sidewall differences are likely due to the absence of sidewall recirculation in the QUIC-URB wind solution.

On the rooftop, the predicted value of the coefficient of pressure varies from -0.8 at the windward side to +0.6 at the leeward side, whereas the wind-tunnel measurements show a uniform value of about -0.6. On the back face, the predicted mean pressure value shows a lateral variation from -0.7 at the wall edges to about -0.45 at the center, whereas the experimental data shows a uniform value of about -0.55.

For both the rooftop and back face, where there is a large gradient in the Reynolds stress, the disagreement between model and measurements may be due to neglecting the Reynolds stresses in the pressure solver. Or the differences may be due to poor representation of the mean flow in these regions by the QUIC-URB wind model.

To understand the significance of the differences between the model output and the measurements, we have also looked at the pressures measured on a cube as reported in the ASHRAE Handbook (1985) and the pressures computed by a large-eddy simulation (LES) model. As one can see when comparing Figs. 2 and 4, there are significant differences between the two experimental data sets. Although the measurements on the front face agree almost perfectly, the  $C_p$  values measured on the rooftop, back face, and sidewall are significantly smaller in magnitude for the ASHRAE case.

LES simulations performed by Rehm et al. (1999) show that even much more sophisticated wind models do not match the experimental pressure measurements that well for some of the walls (Fig. 5). Although there is reasonable agreement with the Baines data on the front face and sidewall, there are appreciable differences on the rooftop and back wall. In fact, the rooftop values are similar to those computed by the QUIC Pressure Solver (see Fig. 2).

#### *ii. Shear flow normal to the cube face*

To match the Baines shear-flow experiment, a power-law inlet velocity profile was specified in the QUIC simulation (see Eqn. (5)). The reference velocity  $u_{ref}$  at building height was set to 5m/s. The value of the power-law index  $n$  was taken as 0.25. The rooftop recirculation and the upwind cavity flags were turned on in the QUIC-URB wind model. The grid cell size was again set to  $H/10$ . The reference height for normalizing pressure was again taken as the building height ( $H$ ).

Figure 6 shows the pressure coefficient contours generated by the QUIC Pressure Solver on the building surfaces and Figure 7 shows the wind-tunnel measurements (Baines, 1963). The predicted and measured  $C_p$  on the front face has a somewhat similar spatial distribution, although there are some significant differences especially over the lower half of the building face. The maximum value on the front face is under predicted by about 15% and is found higher up on the building face. The differences on the lower half of the building face may result from the pressure solver neglecting the Reynolds stresses which have high gradients there. In addition, the differences may be due to differences between the model-produced and measured mean wind in the upwind cavity zone.

On the rooftop, the model-computed and measured  $C_p$  both vary from large negative values just downwind of the leading edge and increase as the back edge is approached. The

model computations tend to have stronger spatial gradients near the leading and back edges and weaker spatial gradients in the middle of the roof. The maximum pressure deficit found near the leading edge is over predicted by about 25%, while positive values are found in the model solution near the back edge in contrast to the negative values obtained in the measurements.

As previously mentioned, due to QUIC-URB not producing sidewall recirculation zones, we expect significant differences between model-computed and measured  $C_p$  values. Larger pressure deficits are found in the measurements, with  $C_p$  values being about 2-4 times those predicted by the pressure solver.

The pressure deficit computed by the QUIC Pressure Solver on the back wall is substantially larger as compared to the experimental data. The predicted values show a variation from -0.5 to -0.35 on the back wall whereas the measured values have a more uniform value of -0.2 on the back wall.

As we did earlier, we also show results from a model simulation performed by Rehm et al. (1999) using the more advanced LES technique. Figure 8 shows that for the shear flow case that the LES model performs much better as compared to the uniform flow case, although the results are not in complete agreement with the experimental data. For example, the LES simulation underestimates the maximum pressure deficit on the sidewall by about 20% (a model-computed  $C_p$  of -0.65 compared to a measured value of -0.8) and the LES simulation values of mean pressure coefficient on the back wall are somewhat lower than the experimental data.

#### *iii. Uniform flow at an angle of 45 degrees to the cube face*

For the last comparison, we have used measurements reported in the ASHRAE Handbook (1985). The inflow for QUIC-URB was specified to be at an angle of 45 degrees relative to building face and uniform with height at 5 m/s. As in the first case, the upwind cavity flag in QUIC-URB has been turned off to better match the experimental flow. Likewise, the rooftop recirculation parameterization has been turned on. As in the previous two cases, the grid cell size was set to  $H/10$  and the reference height for normalizing pressure was taken as the building height ( $H$ ).

Figure 9 shows the model-computed mean pressure coefficient on the building surfaces and Fig. 10 shows the measurements from the

ASHRAE Handbook. It is observed that the mean pressure values predicted by the QUIC Pressure Solver are in good agreement with the ASHRAE handbook data on the upwind faces and on the rooftop. The spatial distributions on these faces are in good agreement too. The predicted values on the front walls vary laterally from 0.9 to -0.4, while the ASHRAE data vary from 0.9 to 0.0. The predicted values of coefficient of pressure on the rooftop are in fairly good agreement with the measured values. The predicted values show formation of two separated low pressure regions having value -0.5, which is also observed in the ASHRAE data. The slight asymmetry seen in the values of  $C_p$  on the rooftop is due to a slightly asymmetric wind field produced by the QUIC-URB wind model during the process of converting from a staggered grid system to a cell-centered one.

The mean pressure values computed by the QUIC Pressure Solver on the back walls are not in agreement with the experimental data. The predicted values of  $C_p$  are substantially lower (more negative) than the experimental data. This may be due to poor representation of the mean wind field by QUIC-URB in the cavity region or it may be due to the effect of Reynolds stresses which have been neglected in the pressure solver.

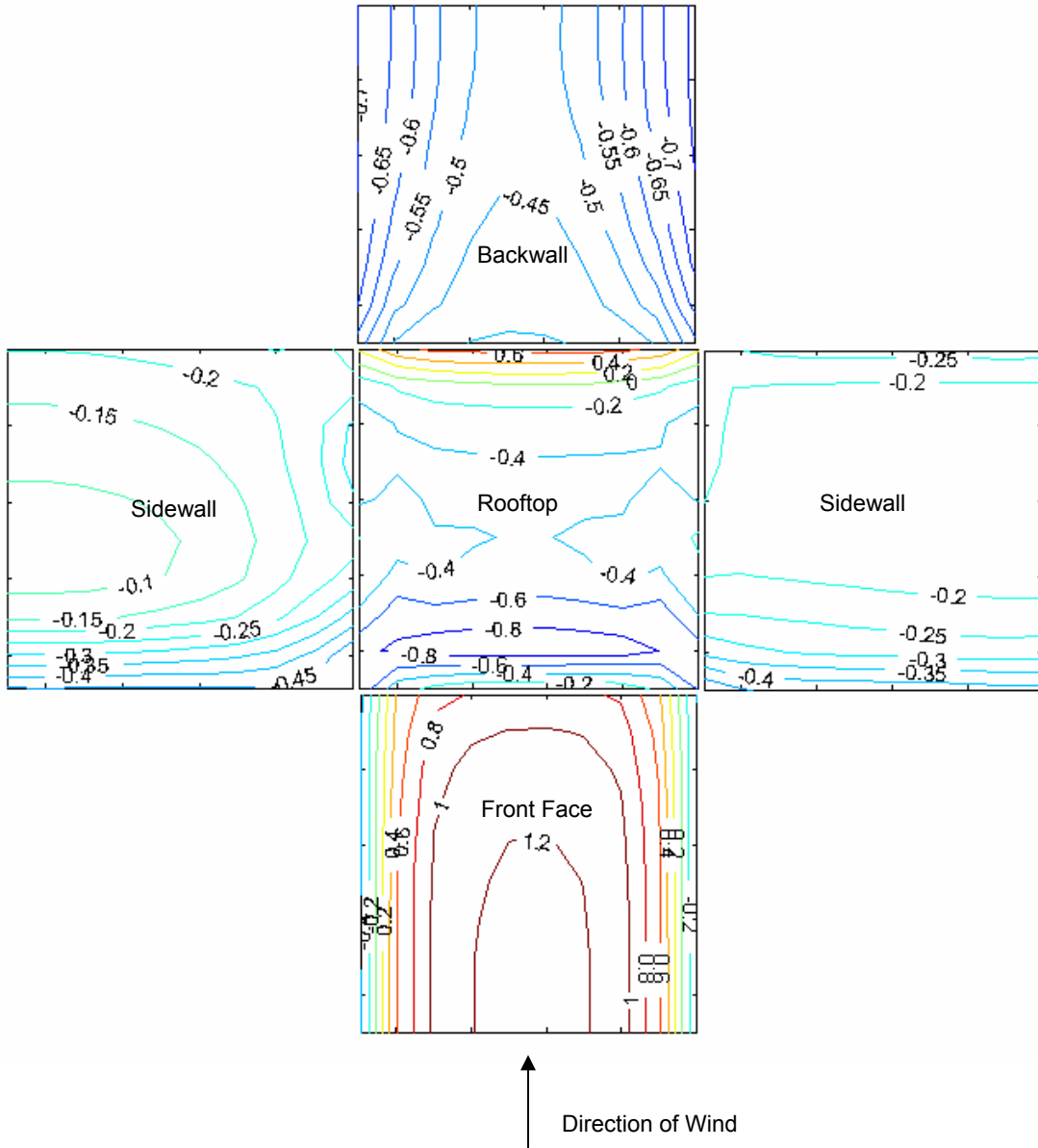


Fig. 2: Pressure coefficient produced by the QUIC Pressure Solver on a cubical building for a uniform inflow perpendicular to the building face.

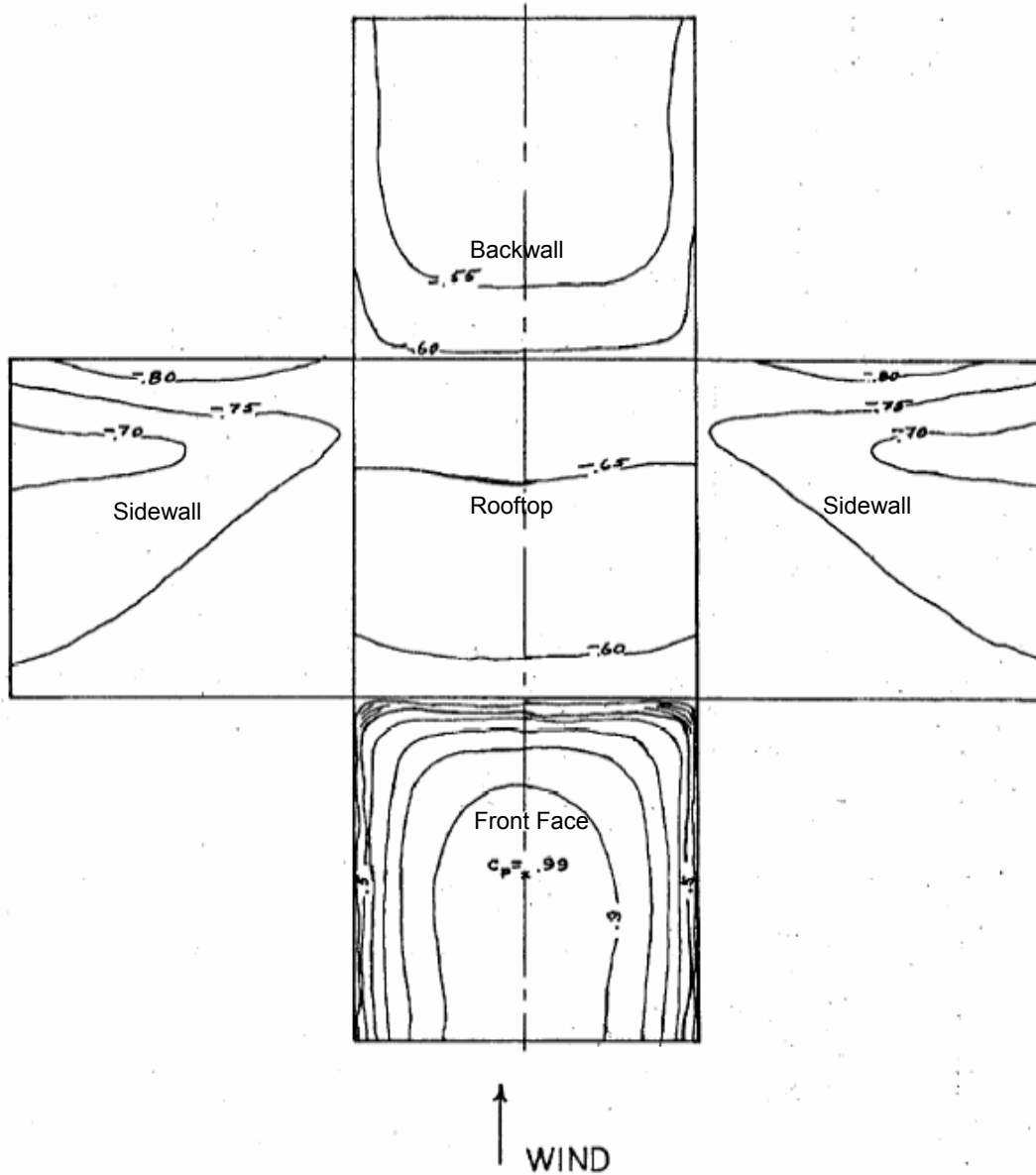


Fig. 3: Wind-tunnel measurements of the pressure coefficient on a cubical building for a uniform inflow perpendicular to the building face (from Baines, 1963).

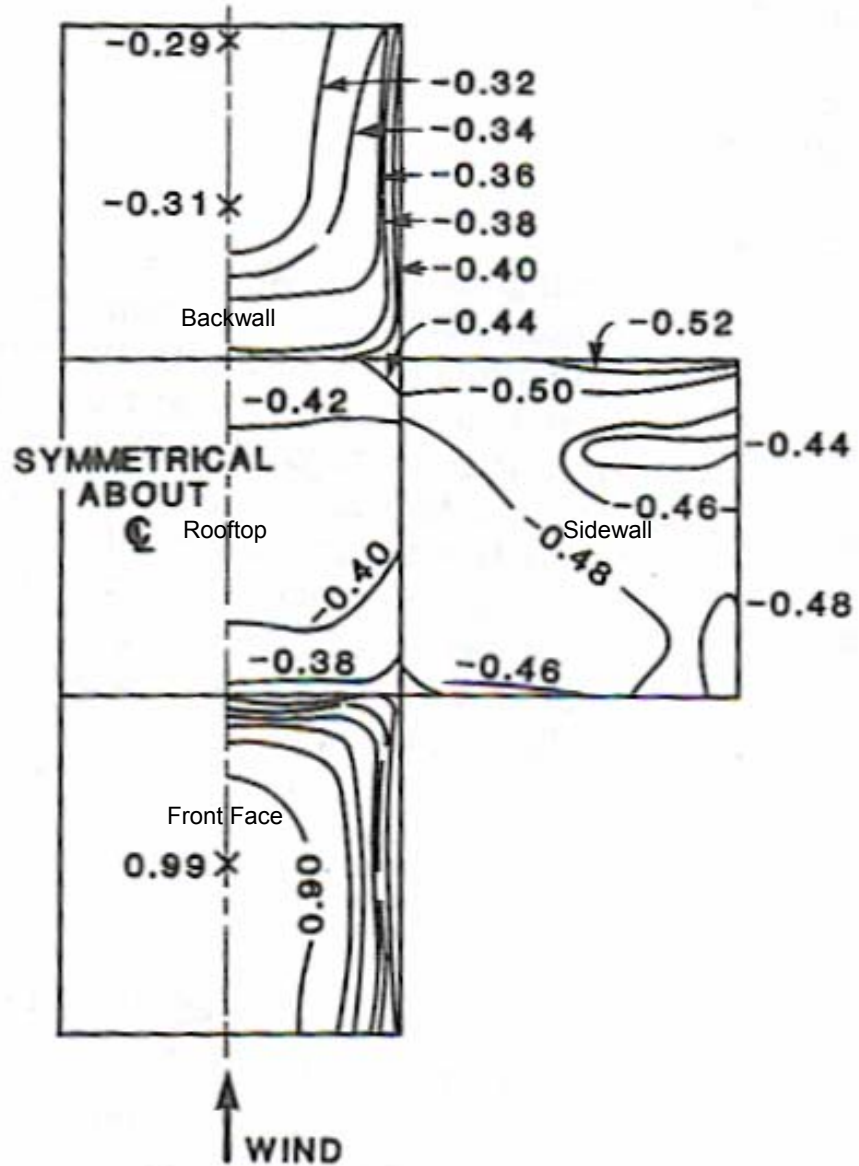


Fig. 4: Pressure coefficient measured on a cubical building with uniform inflow perpendicular to the building face (from ASHRAE handbook, Chap.14, p.14.4).

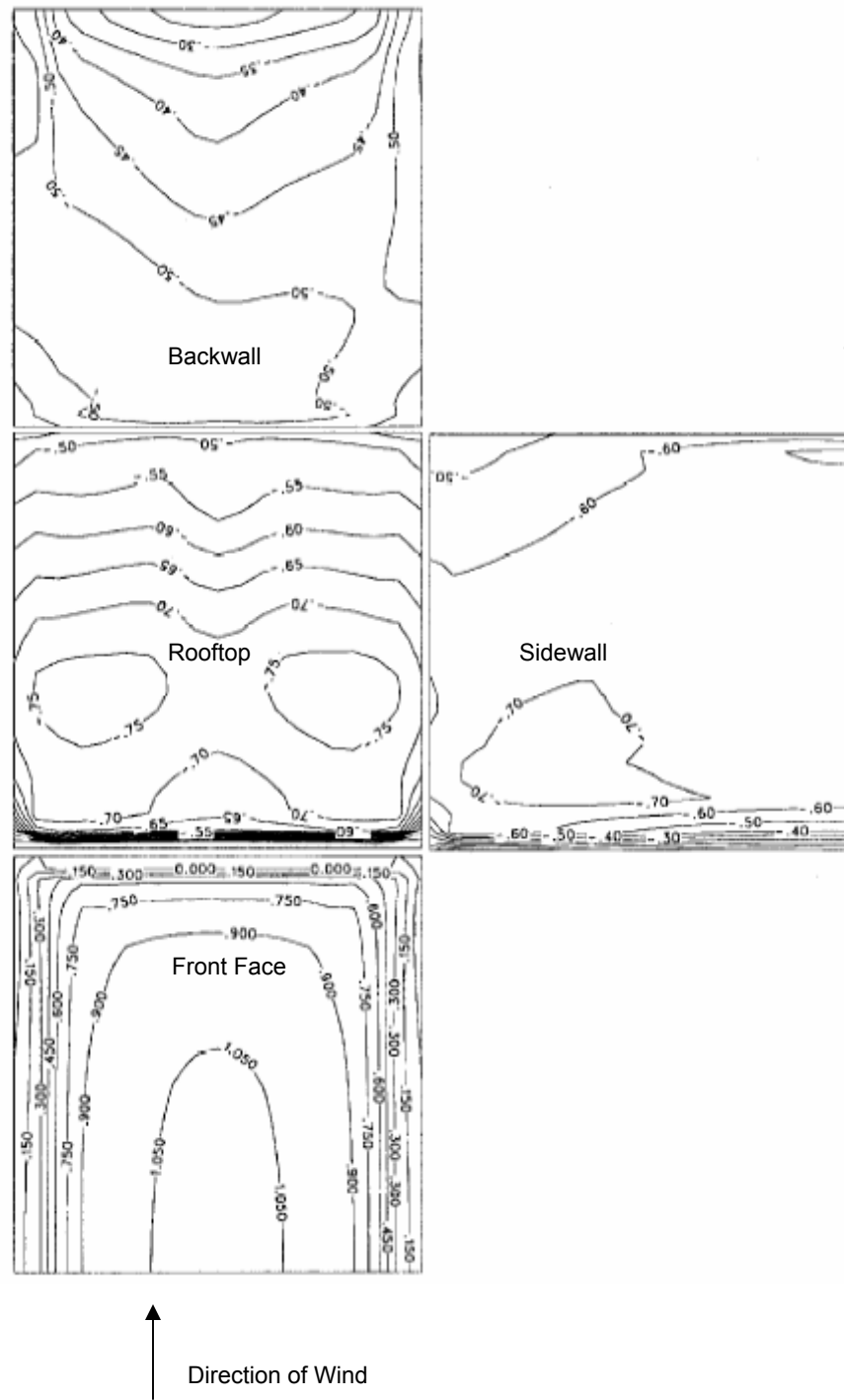


Fig. 5: Average pressure coefficient computed by an LES model for a cubical building with uniform inflow perpendicular to the building face (from Rehm et al., 1999).



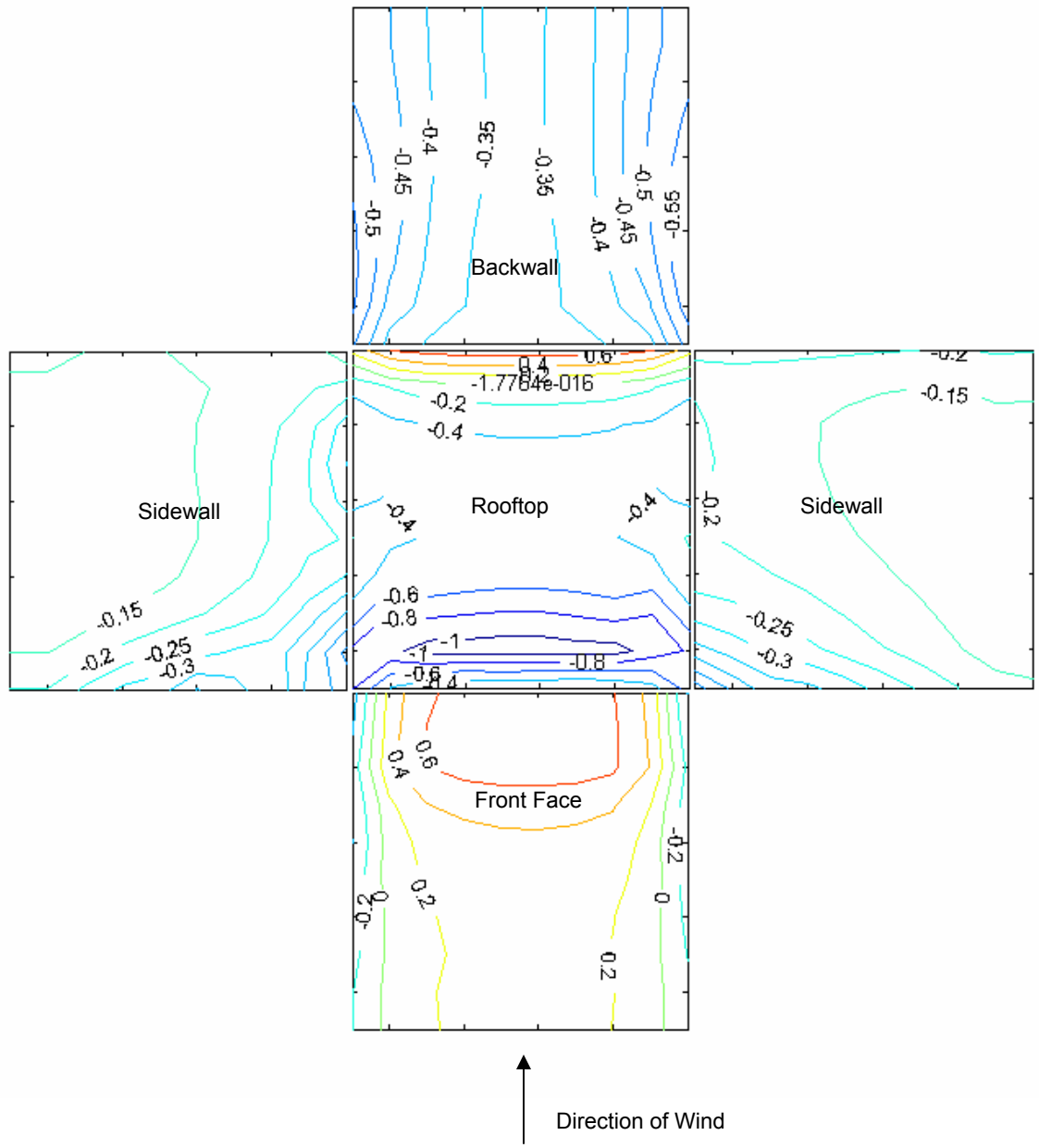


Fig. 6: Pressure coefficient produced by the QUIC Pressure Solver on a cubical building for a shear inflow perpendicular to the building face.

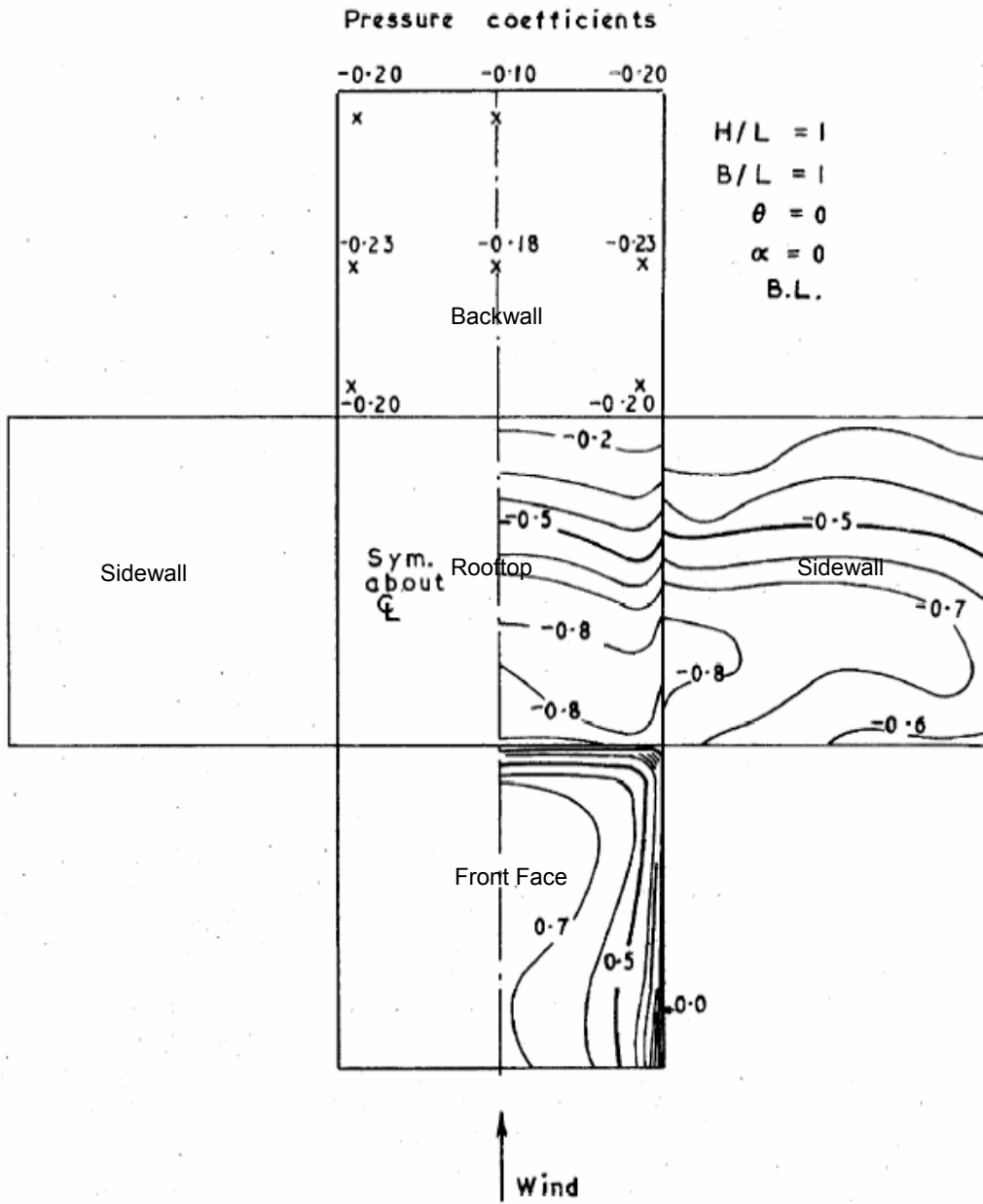


Fig. 7: Wind-tunnel measurements of the pressure coefficient on a cubical building for a shear inflow perpendicular to the building face (from Baines, 1963).

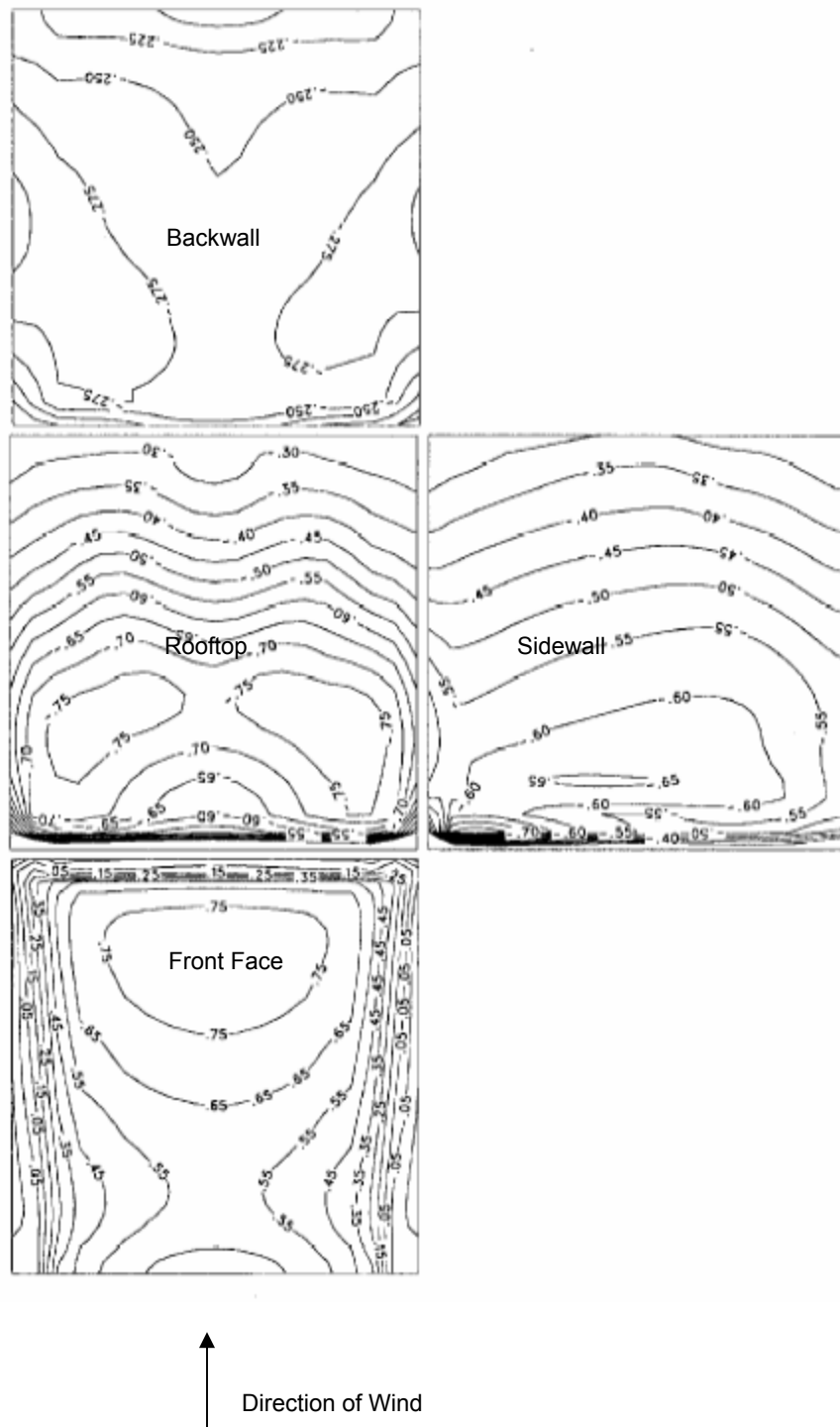


Fig. 8: Average pressure coefficient computed by an LES model for a cubical building with shear inflow perpendicular to the building face (from Rehm et. al., 1999).

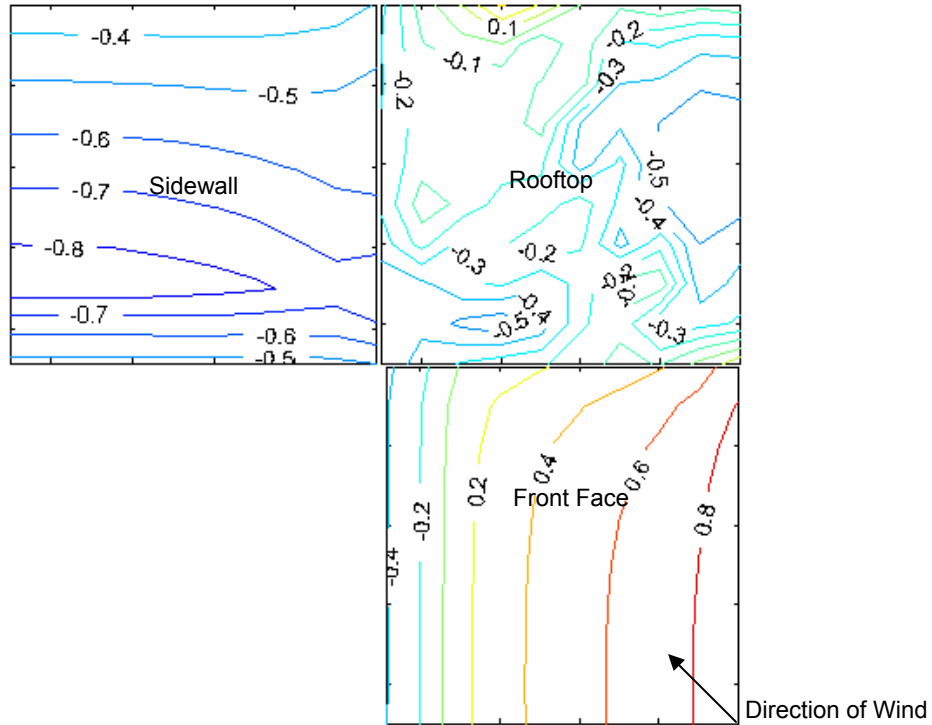


Fig. 9: Pressure coefficient produced by the QUIC Pressure Solver on a cubical building for a uniform flow of 5 m/s at an angle of  $45^\circ$  to the building face.

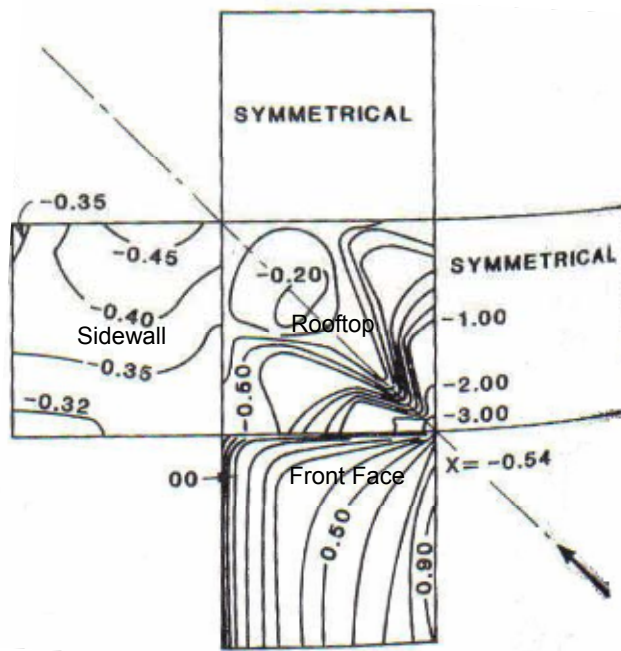


Fig. 10: Pressure coefficient for a uniform flow of over a cubical building at an angle of  $45^\circ$  to the building face (from ASHRAE handbook, Chap.14, p.14.4).

## 5. CONCLUSION

In this paper, we have compared the pressure coefficient  $C_p$  computed by the QUIC Pressure Solver to experimental measurements on a cube for three different flow types. It has been observed that the model-computed  $C_p$  is in reasonably good agreement with the experimental data on the upwind face of the cubical buildings in spite of neglecting the Reynolds stresses in the pressure solver. This is because the pressure gradients in this region are mostly dominated by the mean inflow.

The mean pressure values computed by the model on the rooftop face are in fair agreement with the experimental data. For the case where the incident wind is normal to the building face, the model clearly shows a large pressure deficit on the windward side of the rooftop which is due to separation and suction caused by rooftop recirculation and the negative pressure decreases as we go from the windward side to leeward side.

The predicted values of  $C_p$  on the back face of the building are not consistent with the experimental data. However, there are also significant differences between experimental data from two different sources and results from LES simulations.

The model is not able to predict  $C_p$  correctly on the sidewalls of the building due to the lack of a side-wall recirculation zone in the QUIC-URB wind model. The model appears to perform slightly better for the oblique wind angle case and for the shear inflow case.

In summary, the mean pressure coefficient predicted by the QUIC Pressure Solver is in fair to reasonable agreement on the front and rooftop faces for a cube, in worse agreement on the back face, and in poor agreement on the side face. It is expected that if the mean wind fields computed by the QUIC-URB model are improved that the pressure solutions will also improve. QUIC-URB is currently undergoing testing and evaluation and a side-wall recirculation algorithm is planned to be implemented in the near future. We also intend to investigate the effects of neglecting the Reynolds stresses in our calculations and to ascertain what sorts of errors are acceptable for emergency response applications, for example, outdoor-to-indoor infiltration.

## 6. REFERENCES

Architectural Institute of Japan, 1998: Numerical prediction of wind loading on buildings and structures.

ASHRAE Handbook of Fundamentals, 1985 ed., p. 14.4, American Society of Heating, Refrigerating and Air-Conditioning Engineers, Inc., Atlanta, GA, 1985

Baines, W.D., 1963: Effects of velocity distribution on wind loads and flow patterns on buildings. *The symposium on wind effects on buildings and structure*, Middlesex, England, National Physical Lab. **1**, 197-225.

Gowardhan, A.A., Brown, M.J. and DeCroix, D.S., 2005: QUIC Pressure Solver- *A technical Report*, Los Alamos National Laboratory, Los Alamos, NM.

Pardyjak, E.R. and M.J. Brown, 2001: Evaluation of a Fast-Response Urban Wind Model- Comparison to Single-Building Wind Tunnel Data. Los Alamos National Laboratory report LA-UR-01-4028.

Rehm, R.G., McGrattan, K.B., Baum, H.R. and Simiu E., 1999: An efficient large eddy simulation algorithm for computational wind engineering: Application of surface pressure computation on a single building.. National Institute of Standards and Technology report NISTIR 6371.

Röckle, R., 1990: Bestimmung der stromungsverhältnisse im Bereich Komplexer Bebauungsstrukturen. Ph.D. thesis, *Vom Fachbereich Mechanik, der Technischen Hochschule Darmstadt*, Germany.